

Dehydrogenation of Simple Hydrocarbons on Platinum Cluster Ions

Tetsu Hanmura,[†] Masahiko Ichihashi,[‡] and Tamotsu Kondow^{*,‡}

East Tokyo Laboratory, Genesis Research Institute, Inc., 717-86 Futamata, Ichikawa, Chiba 272-0001, Japan, and Cluster Research Laboratory, Toyota Technological Institute in East Tokyo Laboratory, Genesis Research Institute, Inc., 717-86 Futamata, Ichikawa, Chiba 272-0001, Japan

Received: May 22, 2002; In Final Form: September 13, 2002

Reactions of size-selected platinum cluster ions, Pt_n^+ ($n = 1-5$), with small hydrocarbon molecules (CH_4 , C_2H_6 , C_2H_4 , and C_2H_2) were studied in a beam-gas cell geometry at collision energies less than 1 eV employing a tandem mass spectrometer. It was found that dehydrogenation of the hydrocarbon molecules proceeds exclusively on Pt_n^+ and the absolute cross sections of the reactions depend critically on the cluster size, n , and the collision energy. The size- and the collision energy-dependent cross sections are successfully explained in an RRK framework.

1. Introduction

Platinum is one of the most useful elements in many catalytic reactions such as hydrogenation, dehydrogenation, and cracking of various hydrocarbons.^{1,2} In practical catalysts, platinum is frequently dispersed on a solid support as fine particles whose reactivity depends critically on their diameters.³ It has been reported, for instance, that the rate of hydrogenation of ethylene on platinum particles increases as the particle diameters decrease down to ~ 0.6 nm,^{4,5} which corresponds to the cluster size (the number of the constituent platinum atoms) of ~ 10 . There has been no further study on the catalytic activity of platinum particles with smaller sizes although dramatic size-dependent catalysis is expected in this size region, probably because of difficulty of preparing and identifying such small particles accurately. To overcome this difficulty and unveil such size-specific reactivity, a totally different approach should be contrived and introduced. In such an approach, it is desirable that the reaction be conducted on a size-selected platinum cluster or its ion, which is free of any environmental effects due to liquid media, solid supports, etc. Studies of this kind are realized in a collision reaction of a size-selected platinum cluster ion with a reactant molecule in the gas phase.

Several groups have so far experimentally investigated reactions of Pt^+ with hydrocarbons.⁶⁻¹⁴ Reactions involving platinum cluster ions, Pt_n^+ , with small molecules also have been explored.^{13,15-18} These reactions have been performed mainly under conditions that the cluster ions collide with reactant molecules many times before the product ions are sampled, and in some cases the rate constants of the overall reactions have been obtained from the intensity decrease of the parent ion. For instance, Bondybej and co-workers have measured the rate constants of dehydrogenation of methane by Pt_n^+ ($n = 1-9$) in a Fourier transform ion cyclotron resonance (FT-ICR) mass spectrometer; the rate constant generally increases and approaches to the collision rate as the cluster size increases, but has a minimum at the size of 4.¹³ Michl and co-workers have investigated dehydrogenation and cracking of *n*-butane by Pt^+ and Pt_2^+ under a single collision condition in a triple-quadrupole

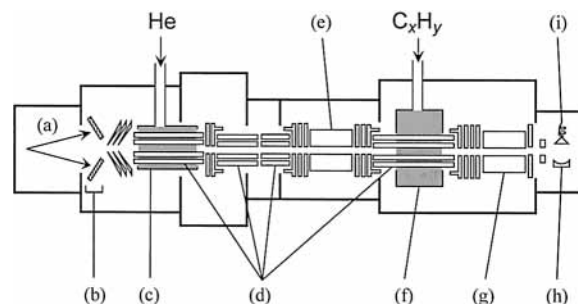


Figure 1. Schematic view of the apparatus: (a) xenon ion beam, (b) platinum targets, (c) cooling cell, (d) octopole ion guides, (e) first quadrupole mass filter, (f) collision cell, (g) second quadrupole mass filter, (h) ion conversion dynode, and (i) secondary electron multiplier.

mass spectrometer.¹⁵ On the other hand, Morokuma and co-workers have calculated the geometric structures of platinum clusters (dimer and trimer) adsorbed with methane by using a density functional method.^{19,20}

In the present study, we measured the absolute cross sections for the reactions of size-selected Pt_n^+ ($n = 1-5$) with CH_4 , C_2H_6 , C_2H_4 , and C_2H_2 , under a single collision condition, to investigate the initial catalytic processes induced by the collision. We have found that one hydrogen molecule is liberated by the collision (the initial step of dehydrogenation on Pt_n^+), and the dehydrogenation cross sections are extremely large and size-dependent.

2. Experimental Section

The apparatus employed in the present study is described briefly in this report (see refs 21–23 for detailed descriptions). A schematic diagram of the apparatus is shown in Figure 1. The apparatus consists of a cluster ion source, a cooling cell, quadrupole mass filters, a collision cell, and a detector. Platinum cluster ions were produced by xenon-ion sputtering on four platinum targets mounted circularly with respect to the xenon ion beam produced from a plasma ion source²⁴ (CORDIS Ar25/35c, Rokion Ionenstahl-Technologie); the energy of the xenon ion is increased up to 18 keV. The cluster ions were cooled in the first octopole ion guide filled with helium gas having a pressure of 10^{-3} Torr and a temperature of 300 K, and were

* Corresponding author. E-mail: kondow@mail.cluster-unet.ocn.ne.jp.

[†] East Tokyo Laboratory, Genesis Research Institute, Inc.

[‡] Cluster Research Laboratory, Toyota Technological Institute.

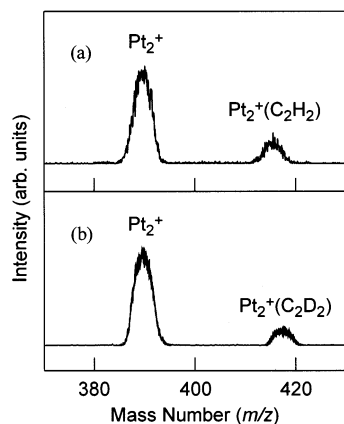


Figure 2. Mass spectra of ions produced by the collision of Pt_2^+ with (a) C_2H_4 and with (b) C_2D_4 at the collision energy of 0.15 eV. The peak assignment is given.

then transported into the first quadrupole mass filter for size-selection of the cluster ions. A size-selected platinum cluster ion from the mass filter was admitted into the octopole ion guide surrounded with a collision cell in which reactions between the platinum ion and a reactant molecule under controlled collision energies take place. Commercially available reactant gases, CH_4 , C_2H_6 , C_2H_4 , C_2D_4 , and C_2H_2 , were used without further purification. A spinning rotor gauge (MKS, SRG-2) measured the pressure in the collision cell. To fulfill the single-collision condition, the pressure in the collision cell was maintained at $\sim 5 \times 10^{-5}$ Torr. The product ions from the collision cell were mass-analyzed in the second quadrupole mass filter and were detected by a detector consisting of an ion conversion dynode and a secondary electron multiplier (Murata Ceratron, EMS-6081B). The signal from the detector was processed in an electronic circuitry based on a personal computer. The spread of the translational energy of the parent cluster ions was determined to be typically 5 eV in the laboratory frame by applying a retarding voltage to the octopole ion guide mounted in the collision cell. This energy spread gives rise to the uncertainty of about ± 0.1 eV in the center-of-mass frame in a collision involving a platinum tetramer ion.

The total reaction cross section, σ_r , is expressed as

$$\sigma_r = \frac{k_B T}{Pl} \ln \frac{I_r + \sum I_p}{I_r} \quad (1)$$

where I_r and $\sum I_p$ represent the intensity of a parent ion passing through the collision region and the sum of the intensities of the product ions, respectively, P and T are the pressure and the temperature of a sample gas, respectively, l ($= 120$ mm) is the effective path length of the collision region, and k_B is the Boltzmann constant.

3. Results

Figure 2 shows typical mass spectra of $\text{Pt}_2^+(\text{C}_2\text{H}_2)$ and $\text{Pt}_2^+(\text{C}_2\text{D}_2)$ produced by the collision of Pt_2^+ with C_2H_4 (panel a) and C_2D_4 (panel b) together with intact Pt_2^+ passing through the collision cell. The peaks of the mass spectra are broad because (1) the mass resolution is traded off with the peak intensity and (2) each peak consists of possible combinations of stable isotopes of Pt. It is evident from the mass spectra that dehydrogenation is the only process that takes place on Pt_2^+ . The mass spectra of the other product ions show that all the hydrocarbon molecules studied undergo dehydrogenation in the entire size and collision energy range studied. It has been

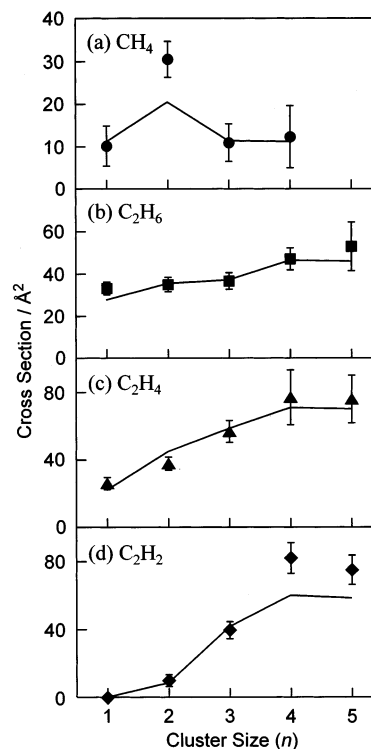
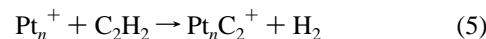


Figure 3. Dehydrogenation cross sections of (a) CH_4 , (b) C_2H_6 , (c) C_2H_4 , and (d) C_2H_2 on Pt_n^+ at the collision energy of 0.15 eV as a function of the cluster size. The symbols (solid circles, solid squares, solid triangles, and solid diamonds) represent the experimental cross sections, and the solid lines are the calculated cross sections (see text). The error bars give one standard deviation of the cross sections experimentally obtained.

reported also that the dehydrogenation is the dominant process in the collision of a platinum ion and platinum cluster ions with hydrocarbons.^{6,11–14} The dehydrogenation is expressed as



The mass peaks were assigned by taking advantage of the fact that the width and the shape of a peak assigned to a given product ion are practically the same as that assigned to the corresponding parent ion. Then, the mass difference of the parent (Pt_n^+) and the product-ion peak gives the mass of an extra species attached to Pt_n^+ . For instance, the product ions due to the reactions of Pt_n^+ with C_2H_4 and C_2D_4 are assigned to $\text{Pt}_n^+(\text{C}_2\text{H}_2)$ and $\text{Pt}_n^+(\text{C}_2\text{D}_2)$, respectively, because the masses for the peaks of the product ions are larger by 26 and 28, respectively, than that of the parent cluster ion (see Figure 2).

Figure 3 shows the cluster size dependence of the cross sections for the dehydrogenation of CH_4 , C_2H_6 , C_2H_4 , and C_2H_2 at the collision energy of 0.15 eV in the center-of-mass frame; the cross sections were obtained from the parent- and the product-ion intensities by using eq 1. In the present experiment, the cross sections for the saturated hydrocarbon molecules are not sensitive to the cluster-size change except for methane, whose cross section at the cluster size of 2 is exceptionally high. On the other hand, the cross sections for the unsaturated

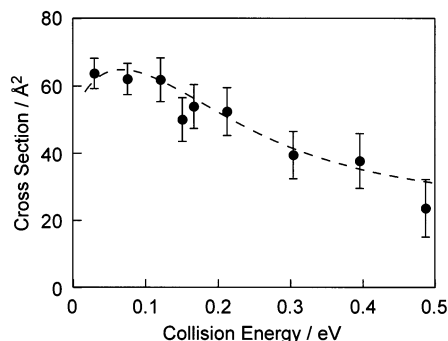


Figure 4. Dehydrogenation cross sections for $\text{Pt}_3^+ + \text{C}_2\text{H}_4$ as a function of the collision energy. The solid circles exhibit the experimental cross sections, and the broken line shows the calculated cross sections (see text). The error bars give one standard deviation of the cross sections experimentally obtained.

hydrocarbon molecules increase rapidly with the cluster size. Figure 4 shows the collision-energy dependence of the dehydrogenation cross section for $\text{Pt}_3^+ + \text{C}_2\text{H}_4$. The cross section decreases with the collision energy similarly to the cross sections for the other reactions studied in the present experiment.

The present cross sections can be compared with those obtained by other groups. Armentrout and co-workers have measured the reaction cross sections for $\text{Pt}^+ + \text{CH}_4$ and CD_4 collisions;¹⁴ the cross sections given in ref 14 are twice as large as ours at the collision energies less than 1 eV, probably because Pt^+ used in the present experiment has a larger energy width. Bondybey and co-workers have measured the rate constants of the $\text{Pt}_n^+ + \text{CH}_4$ reaction in a FT-ICR mass spectrometer.¹³ It is not possible to directly compare our data with theirs because ours are cross sections and theirs are rate constants. The cross sections were converted to our reaction efficiencies defined as the ratio of the reaction cross sections to the Langevin cross section (see Section 4 for the definition of the Langevin cross section) for the comparison with their reaction efficiencies. It was found that the size dependence of our reaction efficiency agrees fairly well with their reaction efficiency except for the size of 3; it is reasonable that the absolute values of ours and theirs do not agree because of the difference of the collision energy used.

4. Discussion

It is conceivable, by analogy to the reaction of Pt^+ with a methane molecule,^{6,8–10,12–14} that dehydrogenation proceeds as

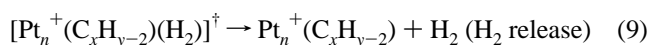
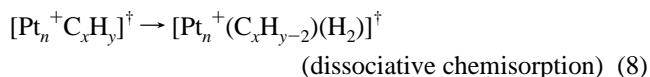


Figure 5 shows a schematic reaction potential, which is simple enough to represent this reaction scheme. Initially, a hydrocarbon molecule, C_xH_y , is captured weakly on a platinum cluster ion, Pt_n^+ , by a charge induced-dipole interaction (physisorption) and is then transferred to a chemisorbed state (chemisorption). The C_xH_y -chemisorbed platinum cluster ion changes into the final product ion via a platinum cluster ion with dissociatively chemisorbed species attached. Along the reaction coordinate,

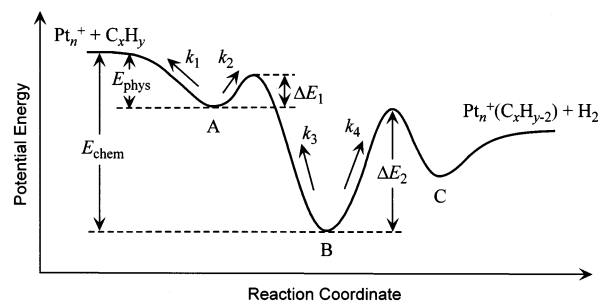


Figure 5. Schematic potential energy curve along the reaction coordinate for the dehydrogenation of C_xH_y on Pt_n^+ . The energy minimums noted as A, B, and C correspond to the physisorbed, the chemisorbed, and the dissociatively chemisorbed states, respectively. See text for the definition of the energy barriers, ΔE_1 and ΔE_2 , and the rate constants.

the reactant system changes into the product system by surmounting the energy barriers of ΔE_1 and ΔE_2 , lying along the reaction coordinate between the physisorbed and the chemisorbed states, and between the chemisorbed and the dissociatively chemisorbed states, respectively.

The dehydrogenation cross sections were estimated by a procedure in which the physisorption cross section is approximated by the Langevin cross section for Pt_n^+ capturing C_xH_y in the charge-induced dipole field, and the subsequent reactions are given in the RRK scheme.²⁵ Suppose that a physisorbed hydrocarbon molecule is either desorbed or chemisorbed by surmounting the energy barrier, ΔE_1 , with the rate constants of k_1 and k_2 , respectively. Further, the chemisorbed hydrocarbon molecule either returns to the physisorbed one with a rate constant of k_3 or proceeds to the dissociatively chemisorbed species with a rate constant of k_4 by surmounting the energy barrier, ΔE_2 . It is assumed that the energetics determines the rate of the dissociatively chemisorbed species into the final product.

The cross section of the physisorption is given by the Langevin cross section, σ_L ,

$$\sigma_L = \pi \left(\frac{2\alpha}{E_{\text{col}}} \right)^{1/2} \quad (10)$$

where α is the polarizability of C_xH_y (2.59 \AA^3 , 4.47 \AA^3 , 4.25 \AA^3 , and 3.33 \AA^3 for CH_4 , C_2H_6 , C_2H_4 , and C_2H_2 , respectively)²⁶ and E_{col} is the collision energy in the center-of-mass frame.²⁷ The largest dehydrogenation cross section studied, which is observed for $\text{Pt}_4^+ + \text{C}_2\text{H}_2$ collision, is predicted well by the Langevin cross section, which should be the upper limit of the physisorption cross section. The cluster size dependence of the dehydrogenation cross section is introduced solely from the rate constants, k_1 , k_2 , k_3 , and k_4 but is not from the Langevin cross section which does not depend on the cluster size, n . The dehydrogenation cross section is calculated from the rate equations for the physisorbed intermediate, the chemisorbed intermediate, and the dehydrogenated product based on the reaction scheme shown in Figure 5. In this scheme, the number density of the chemisorbed intermediate is considered to be sufficiently low that the steady-state approximation is applied. The reaction time ($80 \sim 250 \mu\text{s}$) in the present experiment is sufficiently long that the exponential term turns out to be zero. Furthermore, it is considered that either $k_1 \gg k_2$ or $k_3 \ll k_4$ is true because neither the physisorbed intermediate nor the chemisorbed intermediate was observed. By solving the rate equations under these conditions, one obtains the cross section

of the dehydrogenation, σ , as

$$\frac{\sigma}{\sigma_L} \approx \frac{k_2}{k_1 + k_2} \times \frac{k_4}{k_3 + k_4} \quad (11)$$

RRK theory gives the relations

$$k_1 = A_1 \left(\frac{E_{\text{vib}} + E_{\text{col}}}{E_{\text{vib}} + E_{\text{col}} + E_{\text{phys}}} \right)^{N-1} \quad (12)$$

$$k_2 = A_2 \left(\frac{E_{\text{vib}} + E_{\text{col}} + E_{\text{phys}} - \Delta E_1}{E_{\text{vib}} + E_{\text{col}} + E_{\text{phys}}} \right)^{N-1} \quad (13)$$

where E_{vib} , E_{phys} , E_{col} , and ΔE_1 represent the vibrational energy of the parent cluster ion considered to be $(3n-6)k_B T$, the physisorption energy of $C_x H_y$ on Pt_n^+ , the collision energy, and the energy barrier between the physisorbed and the chemisorbed states, respectively (see Figure 5), A_1 and A_2 are the frequency prefactors related to the $Pt_n^+ - C_x H_y$ dissociation from the physisorption and the transfer to the chemisorption from the physisorption, respectively, and N is the total number of the vibrational modes of $Pt_n^+ C_x H_y$ less the internal modes of $C_x H_y$. The rate constants, k_3 and k_4 , are given by

$$k_3 = A_3 \left(\frac{E_{\text{vib}} + E_{\text{col}} + E_{\text{phys}} - \Delta E_1}{E_{\text{vib}} + E_{\text{col}} + E_{\text{chem}}} \right)^{N-1} \quad (14)$$

$$k_4 = A_4 \left(\frac{E_{\text{vib}} + E_{\text{col}} + E_{\text{chem}} - \Delta E_2}{E_{\text{vib}} + E_{\text{col}} + E_{\text{chem}}} \right)^{N-1} \quad (15)$$

where E_{chem} and ΔE_2 represent the chemisorption energy of $C_x H_y$ on Pt_n^+ and the energy barrier between the chemisorbed and the dissociatively chemisorbed states, respectively, A_3 and A_4 are the frequency prefactors related to the $Pt_n^+ - C_x H_y$ dissociation from the chemisorption and transfer to the dissociative chemisorption from the chemisorption, respectively, and N is the total number of the vibrational modes of $Pt_n^+ C_x H_y$. Throughout the calculation, the prefactors, A_3 and A_4 , are assumed to be the frequencies of the Pt-C stretching vibration (470 cm^{-1}) and the C-H stretching vibration (2940 cm^{-1}) of an ethylene molecule adsorbed on Pt(111) surface,²⁸ respectively.

Using eqs 10–15, one obtains the dehydrogenation cross sections at different collision energies at a given cluster size and internal temperature. Figure 4 shows the experimental (solid circles) and the calculated (broken line) cross sections for dehydrogenation of $C_2 H_4$ on Pt_3^+ as a function of the collision energy. In this calculation, the dependence of the reaction cross section of Pt_3^+ on the collision energy observed was fit to that of the calculated cross section with three adjustable parameters, $E_{\text{phys}} - \Delta E_1$, $E_{\text{chem}} - \Delta E_2$, and A_1/A_2 ; the best-fit values of $E_{\text{phys}} - \Delta E_1$, $E_{\text{chem}} - \Delta E_2$, and A_1/A_2 were obtained to be -0.011 eV , -0.015 eV , and 0.33 , respectively. It is likely that $E_{\text{chem}} - \Delta E_2$ is most sensitively size-dependent because ΔE_2 is related to the decomposition of the hydrocarbon molecule chemisorbed on Pt_n^+ , which is sensitively influenced by the electronic structure of Pt_n^+ . Therefore, the fitting for the other sizes was performed with a single adjustable parameter, $E_{\text{chem}} - \Delta E_2$, while $E_{\text{phys}} - \Delta E_1$ and A_1/A_2 were fixed at the best-fit values obtained for $n = 3$. Figure 3 depicts the cross sections thus calculated at the collision energy of 0.15 eV . Figure 6 shows the parameter, $E_{\text{chem}} - \Delta E_2$, obtained in the calculation as a function of the cluster size. There is a strong correlation between the dehydrogenation cross section and the $E_{\text{chem}} - \Delta E_2$

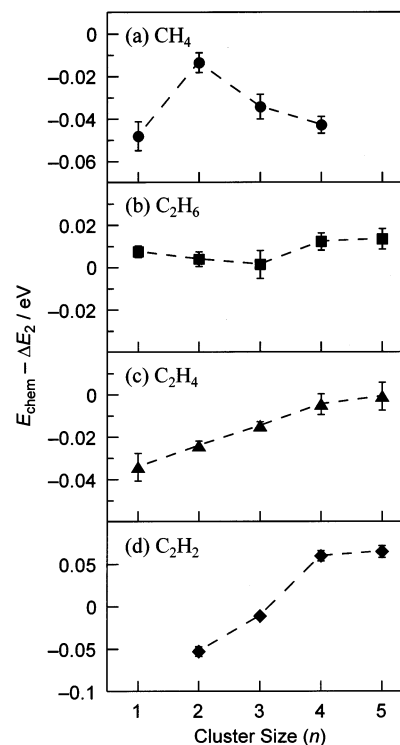


Figure 6. The parameter, $E_{\text{chem}} - \Delta E_2$, for the dehydrogenation of (a) CH_4 , (b) C_2H_6 , (c) C_2H_4 , and (d) C_2H_2 as a function of the cluster size (see text for the definition of E_{chem} and ΔE_2). The errors were estimated from the uncertainties in the fitting.

value; the dehydrogenation cross section is large when the parameter, $E_{\text{chem}} - \Delta E_2$, is large. In other words, the dehydrogenation proceeds more readily when the barrier height, ΔE_2 , is lower.

It is not obvious whether $C_x H_y$ at the chemisorbed state is molecularly chemisorbed as $C_x H_y(a)$, chemisorbed as $C_x H_{y-1}(a) + H(a)$, or otherwise. The calculations of the potential energy surface of the $Pt^+ + CH_4$ reaction have shown that the intermediate is expressed as $H-Pt^+-CH_3$.^{9,10,12,14,29} Morokuma and co-workers have computationally shown that CH_4 on $Pt_{2,3}$ is chemisorbed as CH_3 and H on different Pt atoms.^{19,20} On the other hand, studies on the adsorption of C_2H_4 on Pt(111) surface^{30,31} have revealed that C_2H_4 is at first molecularly adsorbed as π -bonded species below 50 K and then changes into another adsorbate having two $Pt-C$ σ bonds. Finally above 240 K , the adsorbed ethylene decomposes to ethylidyne ($\equiv C-CH_3$) on the surface. These findings suggest that the hydrocarbon molecules studied are also chemisorbed on Pt_n^+ as $C_x H_{y-1}(a)$ and $H(a)$, taking into account that the internal temperature of the chemisorbed intermediates rises as a result of the redistribution of the chemisorption energy. Seemingly, the larger barrier height, ΔE_2 , between the chemisorbed ($Pt_n^+(C_x H_{y-1})(H)$) and the dissociatively chemisorbed states ($Pt_n^+(C_x H_{y-2})(H_2)$) is attributed to difficulty in the abstraction of two hydrogen atoms from $C_x H_y$ on the cluster.

Acknowledgment. This work was supported by Special Cluster Research Project of Genesis Research Institute, Inc.

References and Notes

- Bond, G. C. In *Chemistry of the Platinum Group Metals: Recent Developments*; Hartley, F. R., Ed; Elsevier: Amsterdam, 1991; Chapter 2.
- Sinfelt, J. H. In *Catalysis: Science and Technology*; Anderson, J. R., Boudart, M., Eds; Springer-Verlag: Heidelberg, 1981; Vol. 1, Chapter 5.
- Che, M.; Bennett, C. O. *Adv. Catal.* **1989**, *36*, 55.

- (4) Masson, A.; Bellamy, B.; Colomer, G.; M'bedi, M.; Rabette, P.; Che, M. *Proc. Int. Congr. Catal., 8th* **1984**, 4, 333.
- (5) Masson, A.; Bellamy, B.; Hadj Romdhane, Y.; Che, M.; Roulet, H.; Dufour, G. *Surf. Sci.* **1986**, 173, 479.
- (6) Irikura, K. K.; Beauchamp, J. L. *J. Phys. Chem.* **1991**, 95, 8344.
- (7) El-Nakat, J. H.; Dance, I. G.; Fisher, K. J.; Willett, G. D. *Polyhedron* **1993**, 12, 2477.
- (8) Wesendrup, R.; Schröder, D.; Schwarz, H. *Angew. Chem., Int. Ed. Engl.* **1994**, 33, 1174.
- (9) Heinemann, C.; Wesendrup, R.; Schwarz, H. *Chem. Phys. Lett.* **1995**, 239, 75.
- (10) Pavlov, M.; Blomberg, M. R. A.; Siegbahn, P. E. M.; Wesendrup, R.; Heinemann, C.; Schwartz, H. *J. Phys. Chem. A* **1997**, 101, 1567.
- (11) Taylor, W. S.; Campbell, A. S.; Barnas, D. F.; Babcock, L. M.; Linder, C. B. *J. Phys. Chem. A* **1997**, 101, 2654.
- (12) Achatz, U.; Beyer, M.; Joos, S.; Fox, B. S.; Niedner-Schatteburg, G.; Bondybey, V. E. *J. Phys. Chem. A* **1999**, 103, 8200.
- (13) Achatz, U.; Berg, C.; Joos, S.; Fox, B. S.; Beyer, M. K.; Niedner-Schatteburg, G.; Bondybey, V. E. *Chem. Phys. Lett.* **2000**, 320, 53.
- (14) Zhang, X.-G.; Liyanage, R.; Armentrout, P. B. *J. Am. Chem. Soc.* **2001**, 123, 5563.
- (15) Magnera, T. F.; David, D. E.; Michl, J. *J. Am. Chem. Soc.* **1987**, 109, 936.
- (16) Cox, D. M.; Fayet, P.; Brickman, R.; Hahn, M. Y.; Kaldor, A. *Catal. Lett.* **1990**, 4, 271.
- (17) Kaldor, A.; Cox, D. M. *J. Chem. Soc., Faraday Trans.* **1990**, 86, 2459.
- (18) Jackson, G. S.; White F. M.; Hammill, C. L.; Clark R. J.; Marshall, A. G. *J. Am. Chem. Soc.* **1997**, 119, 7567.
- (19) Cui, Q.; Musaev, D. G.; Morokuma, K. *J. Chem. Phys.* **1998**, 108, 8418.
- (20) Cui, Q.; Musaev, D. G.; Morokuma, K. *J. Phys. Chem. A* **1998**, 102, 6373.
- (21) Ichihashi, M.; Hirokawa, J.; Nonose, S.; Nagata, T.; Kondow, T. *Chem. Phys. Lett.* **1993**, 204, 219.
- (22) Hirokawa, J.; Ichihashi, M.; Nonose, S.; Tahara, T.; Nagata, T.; Kondow, T. *J. Chem. Phys.* **1994**, 101, 6625.
- (23) Ichihashi, M.; Hanmura, T.; Yadav, R. T.; Kondow, T. *J. Phys. Chem. A* **2000**, 104, 11885.
- (24) Keller, R.; Nöhmayer, F.; Spädtkle, P.; Schönenberg, M. H. *Vacuum*, **1984**, 34, 31.
- (25) Draves, J. A.; Luthey-Schulten, Z.; Liu, W.-L.; Lisy, J. M. *J. Chem. Phys.* **1990**, 93, 4589.
- (26) Lide, D. R. *CRC Handbook of Chemistry and Physics*, 78th ed.; CRC Press: Boca Raton, FL, 1997.
- (27) Levine, R. D.; Bernstein, R. B. *Molecular Reaction Dynamics*; Oxford University Press: Oxford, 1974.
- (28) Ibach, H.; Lehwald, S. *J. Vac. Sci. Technol.* **1978**, 15, 407.
- (29) Hada, M.; Nakatsuji, H.; Nakai, H.; Gyobu, S.; Miki, S. *J. Mol. Struct.* **1993**, 281, 207.
- (30) Cremer, P. S.; Somorjai, G. A. *J. Chem. Soc., Faraday Trans.* **1995**, 91, 3671.
- (31) Zaera, F. *Langmuir* **1996**, 12, 88.